Catalysis Letters 29 (1994) 189–207

A corrected procedure and consistent interpretation for temperature programmed reduction of supported MoO_3

John R. Regalbuto [1] and Jin-Wook Ha

Department of Chemical Engineering, University of Illinois at Chicago, 810 S. Clinton, Chicago, IL 60607, USA

Received 15 April 1994; accepted 12 June 1994

Experiments in which bulk MoO_3 has been diluted in silica or alumina reveal a "corrected" TPR pattern in which the bulk oxide reduces at the same temperature as the supported crystalline phase. The reduction patterns for diluted bulk MoO_3, in conjunction with an XRD study of the reduction process and a recent comprehensive speciation theory have greatly assisted the assignment of peaks for silica and alumina supported samples. A simple interpretation of TPR patterns has been applied with good agreement to the body of MoO_3 TPR literature. With consistent interpretation, temperature programmed reduction might be employed with increased confidence to characterize supported MoO_3 and perhaps other supported oxides.

Keywords: MoO_3; molybdena; reduction; temperature programmed reduction; TPR; alumina; Al_2O_3; silica; SiO_2

1. Introduction

Temperature programmed reduction (TPR) has been increasingly employed in the last fifteen years as a simple yet informative characterization technique for supported oxides [1–17]. Among the most studied oxides are molybdena [1–14] and vanadia [16,17]. There currently exists a good deal of complication in the assignment of peaks to species. In earlier works, peaks are generally associated with the complete reduction of a particular species, for example, the low temperature peaks are attributed to the reduction of supported monolayer (over SiO_2) or multilayer (over Al_2O_3) MoO_3 forms, and the higher peak to the reduction of supported MoO_3 crystallites [1,2,4,5,7,8,12]. On the other hand, many recent works have concluded that the reduction of at least some supported MoO_3 species occurs in two separate steps, the first step being $MoO_3 \rightarrow MoO_2$, and the second $MoO_2 \rightarrow Mo$ (metal) [3,6,7,9–11], the latter [11] with a convincing in situ high temperature X-ray

[1] To whom correspondence should be addressed.

diffraction study and another with detailed Raman characterization [9]. In fact, low temperature oxygen chemisorption of supported oxides as developed by Weller, for which citations are too numerous to cite, presumes a $MoO_3 \rightarrow MoO_2 \rightarrow$ Mo reduction sequence.

The majority of the morphological interpretations from TPR data in the above references is incompatible with the rigorous and comprehensive Raman characterization of silica and alumina supported MoO_3 produced by the group of Wachs [9,18–21]. The speciation of supported oxides is now so thorough that it is now couched in terms of a design theory [20,21]. According to this theory, supported oxides exposed to ambient (humid) conditions speciate as if in the liquid phase, at the pH determined by an area weighted average of the isoelectric points of the oxide components. Since the isoelectric points of both silica and MoO_3 are close to 2, silica supported molybdenum exists in the polymolybdate form at any loading. Over alumina, which has an isoelectric point of about 8, molybdena can exist as a monomer at low loadings, and transforms in its entirety to polymolybdate at high loadings. The interpretation of TPR results should correspond to this model of speciation, and since there is no current consistency along these lines, the usefulness of TPR as a characterization technique is called into question.

The assignment of TPR peaks is complicated at the outset by the common observation that the pure bulk oxide reduces at a (much) higher temperature than the supported oxides, even when large crystallites are present on the supports. The concomitant conclusion with regard to morphology is that the supported crystallites are much smaller than the bulk crystals, and the implication in regards to catalytic activity is that the supported crystallites must be easier to reduce than the bulk materials.

The first goal of the present work is to demonstrate that the position of the first reduction peak of bulk MoO_3 can be brought down to about the same temperature as silica or alumina supported MoO_3 crystallites, simply by diluting bulk MoO_3 in either support. This shift is explained by a firmly established mechanism for reduction of bulk molybdena [22]. All TPR results are supported by powder X-ray diffraction taken from TPR runs stopped after a particular peak, to confirm that the diluted bulk as well as the highly loaded impregnated samples undergo the same two-step $MoO_3 \rightarrow MoO_2 \rightarrow$ Mo (metal) reduction process at nearly the same temperature. It is further suggested that, for the silica and alumina supports employed here, the morphology of supported MoO_3 catalysts can be derived from the peaks corresponding to the first $MoO_3 \rightarrow MoO_2$ reduction step. In the case of silica the low temperature peak width appears to be proportional to molybdenum dispersion, and in the case of alumina a second low temperature peak exists.

Secondly, "intrinsic" or "corrected" TPR patterns of bulk oxides obtained by dilution appear to clarify the assignment of peaks for supported samples; with the present interpretation, literature data have been synthesized in a manner that is both largely self-consistent and outwardly consistent with Wachs' speciation model [18–21].

2. Experimental

Catalyst supports employed were Degussa Aerosil (380 ± 30 m^2/g) and LaRouche γ-alumina (130 ± 15 m^2/g). To make handling of the silica easier it was washed with deionized water and dried at 110°C for 12 h, which increased the bulk density several times. Ammonium heptamolybdate(VI) tetrahydrate ($(NH_4)_6Mo_7O_{24}\cdot 4H_2O$, AHM) was purchased from Aldrich.

Supported samples were prepared by physically mixing the appropriate amounts of AHM and support powders, and adding water to incipient wetness. Samples were spread on a watch glass and stirred frequently during drying to minimize Mo migration. Samples were dried in air at room temperature and calcined in air at 500°C for 2 h. Bulk MoO_3 was prepared by calcining pure AHM at the same conditions. This was physically mixed with either support to the desired weight loading. the surface loading of supported MoO_3 catalysts ranged from 0.2 to 4.0 atoms Mo/nm^2 (1.6–27 wt%) for silica, and from 0.6 to 12.0 atoms Mo/nm^2 (1.9–27 wt%) for alumina. The higher surface loadings were needed for the formation of MoO_3 crystallites on the stronger interacting alumina support; it was desired to perform TPR runs with similar MoO_3 morphologies on each support.

In the discussion which follows, "bulk MoO_3" will always refer to the unsupported, very large MoO_3 crystals, while "crystalline MoO_3" will refer to supported crystallites of MoO_3. Physical mixtures of bulk MoO_3 and support will be referred to as "diluted bulk MoO_3".

The TPR apparatus consisted of a 12 mm (o.d.) quartz tube, heated by a split tube furnace. Samples were supported on quartz wool. Gases were purified of O_2 by molecular sieve and indicating oxygen traps. Hydrogen concentration was measured by a thermal conductivity detector. In order to compare the present results with those of other groups, similar TPR conditions were employed; 4 vol% H_2 in N_2 was used at a flow rate of 16.8 sccm. The reactor was mounted vertically and flow progressed downward. After stabilization of the baseline at 400°C, heating began at 5°C/min to 1000°C. Reproduction of the TPR profiles was within a few percent at any particular temperature.

Powder X-ray diffraction was performed with a Siemens D5000 diffractometer operated at 50 kV and 30 mA, using either a backfilled zero background holder or smaller amounts of sample smeared onto a pyrex holder.

3. Results and discussion

3.1. TPR PROFILES OF PHYSICAL MIXTURES

Results from an initial series of physically mixed $MoO_3 + SiO_2$ samples, and pure SiO_2 and MoO_3 are shown in fig. 1. All samples contained 0.2 mmol (29 mg) of MoO_3; physically mixed samples contained MoO_3 in an amount equivalent to 4 atoms Mo/nm^2 SiO_2, or 26.7 wt%. The featureless pattern of SiO_2 is seen in pat-

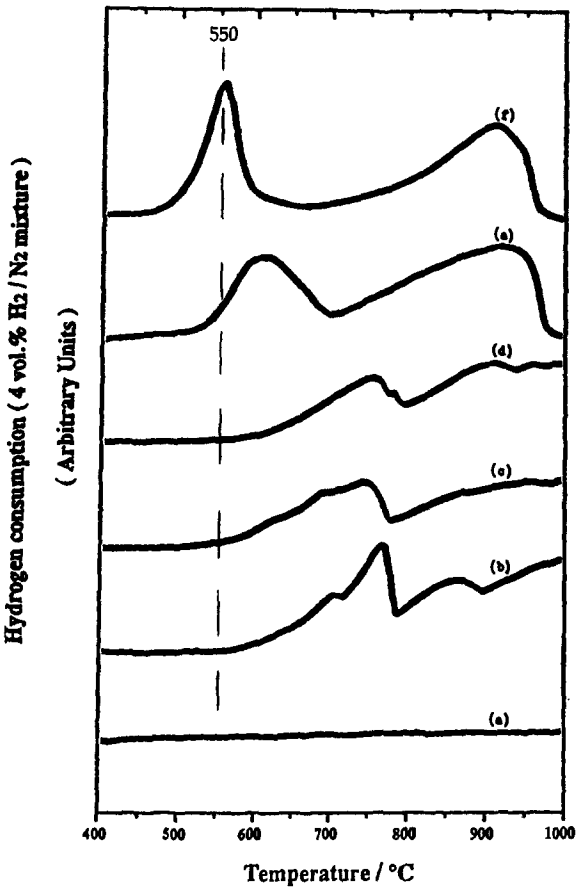

Fig. 1. TPR profiles of physical mixture, orthorhombic $MoO_3 + SiO_2$. Neutral precursor (AHM, impregnated with H_2O (pH = 5)) and air calcination at 500°C for 2 h: (a) SiO_2, (b) bulk MoO_3, and 4.0 Mo/nm^2 physically mixed $MoO_3 + SiO_2$: (c) not mixed (MoO_3 (top), SiO_2 (bottom)); (d) not mixed (MoO_3 (bottom), SiO_2 (top)), (e) roughly mixed, and (f) thoroughly mixed.

tern (a), and pure MoO_3 with the first reduction peak maxima at 770°C in pattern (b). The sample of pattern (c) was made with unmixed MoO_3 powder on top of SiO_2 powder, and pattern (d) with unmixed SiO_2 powder on top of MoO_3. Were water vapor resulting from dehydroxylation of the support to play a role in altering the reduction temperature of MoO_3, patterns (c) and (d) would appear different. However, profiles (b)–(d) are similar; a small amount of interaction is seen in the latter two but the vertical positioning of powders does not greatly affect the patterns. Pattern (e) was produced by mixing the $MoO_3 + SiO_2$ powders with a spatula; the first peak maximum falls to 610°C. Pattern (f) is for a thoroughly mixed sample obtained by grinding in a mortar and pestle for about 15 min; the first reduction peak maximum has fallen to about 550°C. The reduction of both the roughly and thoroughly mixed samples is complete; from the nearly 1 : 2 ratio of peak areas the sequential reduction process $MoO_3 \rightarrow MoO_2$, and $MoO_2 \rightarrow Mo$ is suggested.

TPR profiles from a series of MoO_3 physically mixed with alumina are shown in fig. 2. Once again, the order of vertical positioning is inconsequential in the layered Al_2O_3 and MoO_3 runs, patterns (c) and (d). The first reduction peak maximum of the roughly mixed sample has shifted down to 600°C, pattern (e) and to 540°C for the thoroughly mixed sample, pattern (f). The first temperature peaks for the roughly and thoroughly mixed alumina samples are somewhat broader than the corresponding peaks with SiO_2, which is an indication that peak width increases with increasing strength of interaction. The reduction is not complete in any alumina diluted sample, another symptom of the stronger interaction.

XRD patterns from the thoroughly mixed diluted samples, taken from runs stopped at 650 and 1000°C are shown in figs. 3 and 4 respectively, as patterns (c), for SiO_2, and (f) for Al_2O_3. After the 650°C reduction the pattern of MoO_2 is evi-

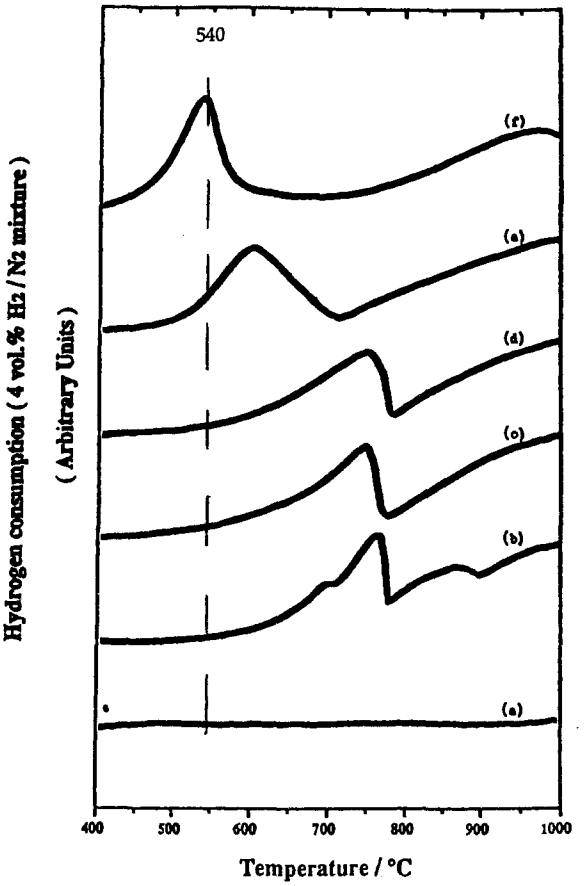

Fig. 2. TPR profiles of physical mixture, orthorhombic $MoO_3 + \gamma\text{-}Al_2O_3$. Neutral precursor (AHM, impregnated with H_2O (pH = 5)) and air calcination at 500°C for 2 h: (a) $\gamma\text{-}Al_2O_3$, (b) bulk MoO_3, and 4.0 Mo/nm^2 physically mixed $MoO_3 + \gamma\text{-}Al_2O_3$: (c) not mixed ($MoO_3$ (top), $\gamma\text{-}Al_2O_3$ (bottom)); (d) not mixed (MoO_3 (bottom), $\gamma\text{-}Al_2O_3$ (top)), (e) roughly mixed, and (f) thoroughly mixed.

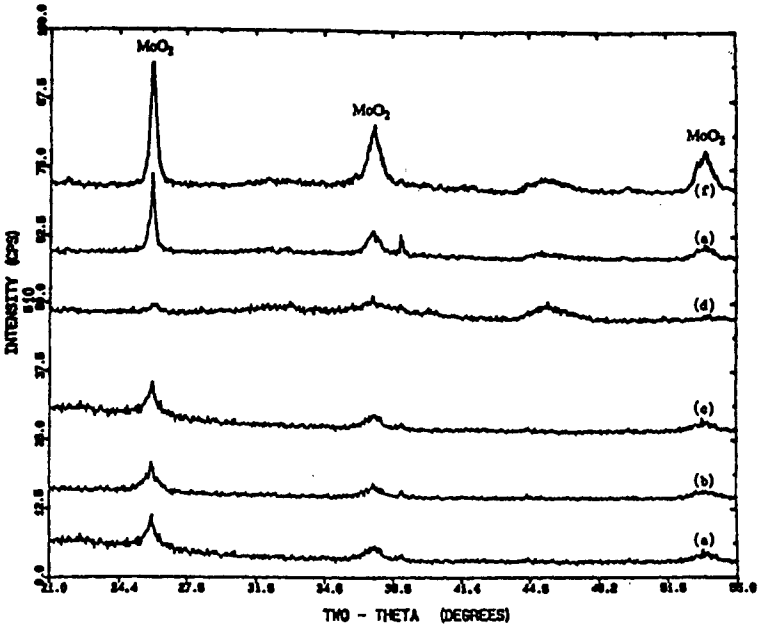

Fig. 3. XRD patterns of both silica and alumina supported MoO_3, reduction to 650°C: (a) 2 Mo/nm^2 MoO_3/SiO_2, (b) 4 Mo/nm^2 MoO_3/SiO_2, (c) 4 Mo/nm^2 $MoO_3 + SiO_2$ (thoroughly mixed), (d) 6 Mo/nm^2 MoO_3/γ-Al_2O_3, (e) 12 Mo/nm^2 MoO_3/γ-Al_2O_3, and (f) 12 Mo/nm^2 $MoO_3 + \gamma$-Al_2O_3 (thoroughly mixed).

dent for these, and for all other impregnated samples to be discussed momentarily. Reduction to elemental Mo at 1000°C occurred in all moderate to highly loaded samples, SiO_2 or Al_2O_3 supported, physically mixed or impregnated, as seen in fig. 4. These XRD findings are similar to a high temperature, in situ XRD study made at slightly different conditions from the TPR experiment [11]. In the present study this reduction pathway is extended to include diluted *bulk* MoO_3.

One other study has performed a TPR experiment with a physical mixture of bulk silica with orthorhombic MoO_3 powder [8]. In that study the mixture was calcined at 500°C after it was mixed. This should have no effect on the morphology, however, as it has been firmly established that bulk orthorhombic MoO_3 physically mixed with silica will not significantly redisperse upon calcination [22]. The first peak T_{max} for the mixed sample was 200°C below that of the pure sample. The authors conclude, typically, that supported Mo(VI) behaves quite differently from unsupported, and in doing so imply that the MoO_3 in the physical mixture redispersed to a considerable extent over the silica surface [8], in contradiction to a wealth of literature (cited in ref. [23]).

If there is no morphological change in MoO_3 (in the untreated mixtures employed here, or in the calcined samples of ref. [8]), what causes the dramatic lowering in reduction temperature in the diluted samples? Gas phase transport limitations would not appear to be the answer. The small grain size of even the bulk

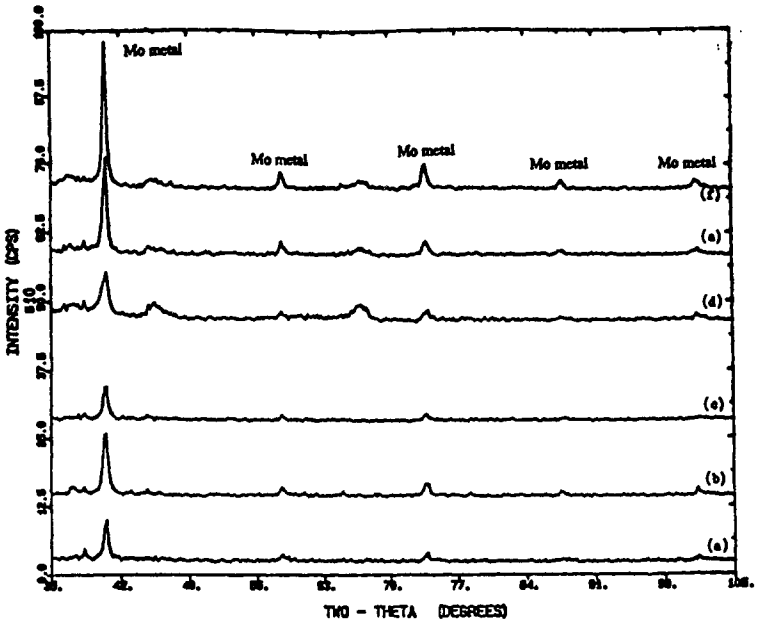

Fig. 4. XRD patterns of both silica and alumina supported MoO_3, reduction to 1000°C: (a) 2 Mo/nm^2 MoO_3/SiO_2, (b) 4 Mo/nm^2 MoO_3/SiO_2, (c) 4 Mo/nm^2 $MoO_3 + SiO_2$ (thoroughly mixed), (d) 6 Mo/nm^2 MoO_3/γ-Al_2O_3, (e) 12 Mo/nm^2 MoO_3/γ-Al_2O_3, and (f) 12 Mo/nm^2 $MoO_3 + \gamma$-Al_2O_3 (thoroughly mixed).

MoO_3 powder samples would prevent external diffusion limitations, and the fact that it is nonporous eliminates the possibility of internal diffusional effects. The parameters of operation are right in the middle of the TPR operating regime recommended by Monte and Baiker [24].

The answer is strongly suggested by the comprehensive work of Arnoldy, de Jonge and Moulijn on the reduction of bulk MoO_3 [22]. First of all they demonstrate a pronounced effect of sample weight on reduction temperature. Increasing the sample weight from 1.2 to 25 mg (fig. 4 of ref. [22]) increases the reduction temperature of the first major peak maxima from about 620 to 820 K which is similar to the shift seen in figs. 1 and 2, and other comparisons of bulk to silica supported MoO_3 reduction [1,6,7,8,11]. A low temperature tail does remain in the high loading sample (pattern f of fig. 4, [22]), and in fact this same feature is observed in the bulk pattern reported by other groups [1,2,4]. The undiluted MoO_3 pattern, (b) in figs. 1 and 2 of the present work, exhibits a tail extending to temperatures below 600°C as well. Arnoldy and coworkers also demonstrate a strong retardation of reduction caused by water vapor [22]. From a series of activation energy determinations, they conclude that the reduction of MoO_3 in these samples occurs by several parallel mechanisms. The low temperature mechanisms are thought to be autocatalytic, involving H_2 dissociation by partially reduced Mo sites, whereas the high temperature pathway is noncatalytic with oxygen diffusion as the rate determining

process. Water inhibits the formation of the catalytic Mo sites; in large MoO_3 samples product H_2O is held up in the bed and retards the low temperature reduction mechanism.

It is plausible that in diluted MoO_3, in which individual crystals are separated from one another by an inert matrix (the volumetric dilution is about a factor of ten), product water vapor is effectively diluted and swept away from the crystals, thus enabling the low temperature reduction mechanism. Supported crystallites and polymolybdates would also undergo this low temperature mechanism, by virtue of being sufficiently dispersed for adequate water removal. The interpretation of TPR patterns for supported samples is given in the next section.

3.2. TPR PROFILES OF IMPREGNATED SAMPLES

That the diluted bulk mixtures unveil a normally inhibited low temperature reduction pathway of bulk oxide particles is further suggested by comparison to the reduction patterns of impregnated samples prepared with large amounts of MoO_3 crystallites. XRD patterns of two series of variable loading SiO_2 (0.2, 0.8, 2, and 4 atoms Mo/nm^2) and Al_2O_3 samples (0.6, 2.4, 6, and 12 atoms Mo/nm^2) are shown in figs. 5 and 6. Crystallites of MoO_3 are noticeable in the next to highest loading in each series, patterns (c) and (d) respectively, and form in large amounts in the highest loading, patterns (d) and (e). Aluminum molybdate also forms in small amounts at the highest Al_2O_3 loading. The reduction pathway of the higher

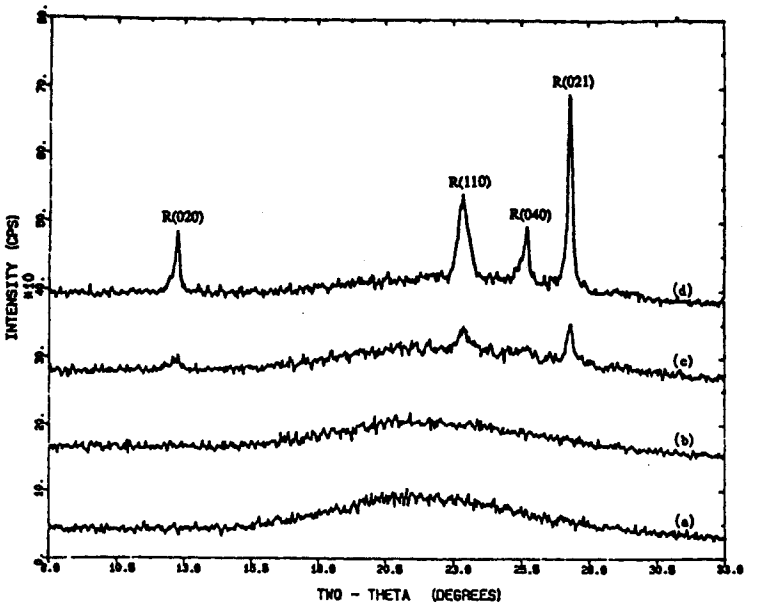

Fig. 5. XRD patterns of neutral precursor (AHM/SiO_2, impregnated with H_2O (pH = 5)) and air calcination at 500°C for 2 h: (a) 0.2, (b) 0.8, (c) 2.0, and (d) 4.0 atoms Mo/nm^2.

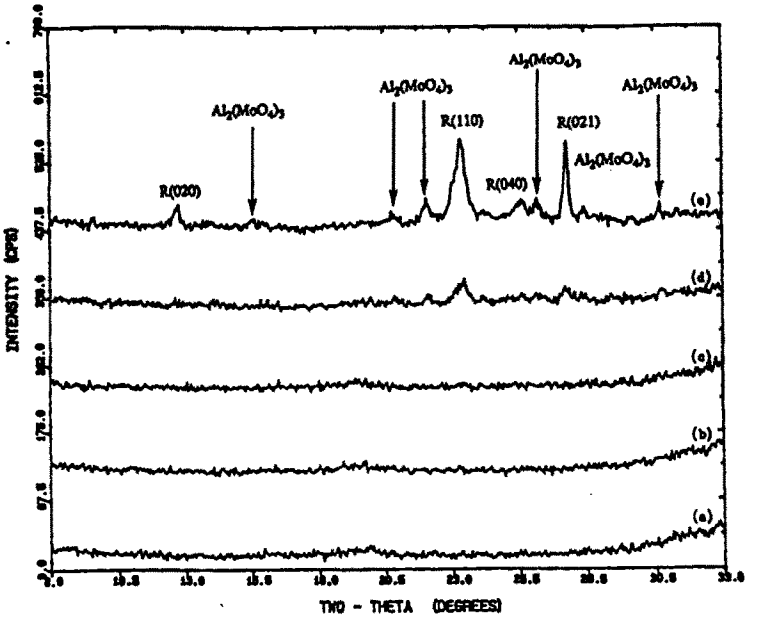

Fig. 6. XRD patterns of neutral precursor (AHM/γ-Al_2O_3, impregnated with H_2O (pH = 5)) and air calcination at 500°C for 2 h: (a) γ-Al_2O_3, (b) 0.6, (c) 2.4, (d) 6.0, and (e) 12.0 atoms Mo/nm^2.

loadings of these two sets of samples have been seen in the previous XRD figures (3 and 4); they follow the same reduction sequence $MoO_3 \rightarrow MoO_2 \rightarrow Mo$ as the physically mixed samples.

TPR patterns for these two series are shown in figs. 7 and 8 for SiO_2 and Al_2O_3 respectively. Each sample again contains 0.2 mmol Mo. Patterns from the thoroughly mixed diluted samples are also included as the top pattern in each figure. For silica, fig. 7, reduction of the lowest loading appears incomplete, which is consistent with the recently postulated particle size effect (stabilization of metallic Mo on silica requires a minimum particle size) reported by de Boer [11]. That is, small MoO_x particles cannot be reduced entirely to Mo metal, such that low weight loadings undergo only the first reduction step $MoO_3 \rightarrow MoO_2$ [11].

At the higher loadings only a single peak is exhibited in the low temperature region, and this peak lines up with the reduction of diluted bulk MoO_3! Only the polymolybdate species should be present on SiO_2, independent of loading, under ambient conditions [18]. The actual reduction process would first involve the dehydration of the polymolybdates, which produces isolated mono-oxo species [25]. The actual process is perhaps best represented as

$$\text{polymolybdate } MoO_3 \xrightarrow[\text{dehydrate}]{} \text{monom-oxo } Mo^{6+} \xrightarrow[\text{reduce}]{} \text{isolated } Mo^{4+}(?) \xrightarrow[\text{rehydrate}]{} MoO_2,$$

however, for brevity in the discussion to follow the convention will be to ad-

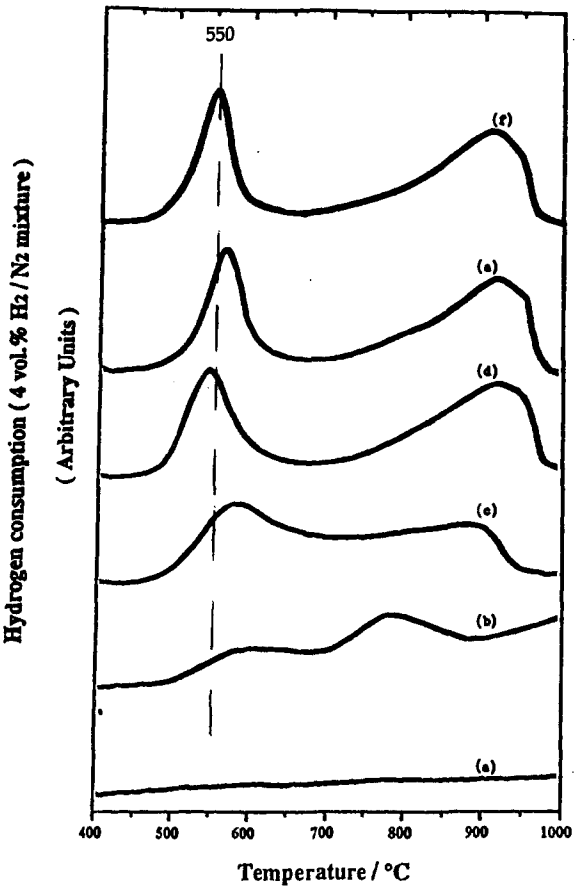

Fig. 7. TPR profiles of neutral precursor (AHM/SiO_2, impregnated with H_2O (pH = 5)) and air calcination at 500°C for 2 h: (a) SiO_2, (b) 0.2, (c) 0.8, (d) 2.0, (e) 4.0 atoms Mo/nm^2 supported MoO_3/SiO_2, and (f) physical mixture of 4.0 atoms Mo/nm^2 $MoO_3 + SiO_2$.

dress the species by its ambient (hydrated) form. The reduction process will be summarized as

$$\text{polymolybdate } MoO_3 \xrightarrow[\text{reduce}]{} MoO_2 .$$

The TPR results in conjunction with XRD (fig. 3) demonstrate that the reduction of well dispersed polymolybdate to MoO_2 occurs at nearly the same rate as supported MoO_3 crystallites $\rightarrow MoO_2$, which in turn occurs at nearly the same rate as appropriately diluted bulk $MoO_3 \rightarrow MoO_2$. All MoO_2 then converts to Mo^0 in the second reduction peak. The reduction mechanism over silica can be described as a simultaneous, parallel pathway for both types of species (polymolybdate and crystalline MoO_3).

A comparison of literature results and interpretations for TPR of silica supported MoO_3 is given in table 1. Here again the shorthand reduction sequence

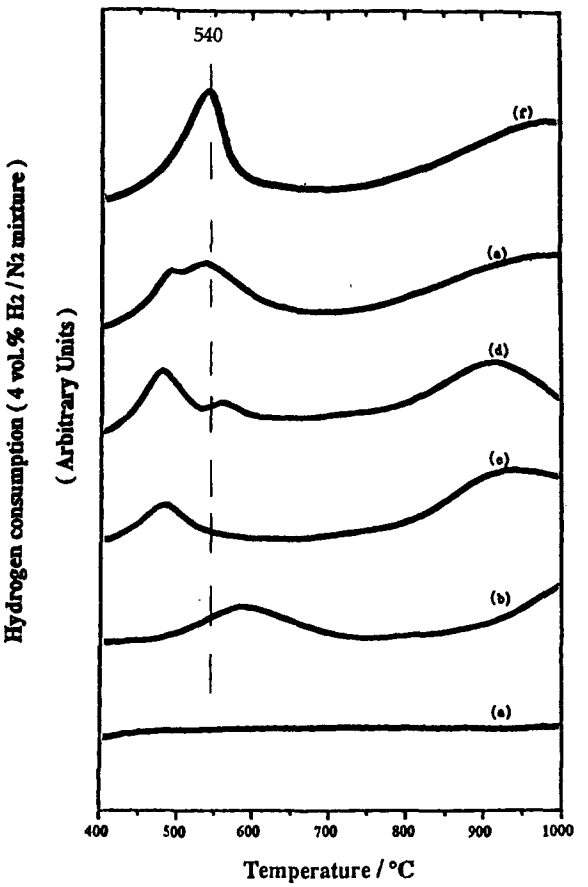

Fig. 8. TPR profiles of impregnated MoO_3/γ-Al_2O_3. Neutral precursor (AHM/γ-Al_2O_3, impregnated with H_2O (pH = 5)) and air calcination at 500°C for 2 h: (a) γ-Al_2O_3, (b) 0.6, (c) 2.4, (d) 6.0, (e) 12.0 atoms Mo/nm^2 supported MoO_3/γ-Al_2O_3, and (f) physical mixture of 12.0 atoms Mo/nm^2 $MoO_3 + Al_2O_3$.

above is used. Similar two-peak reduction patterns for moderate and highly loaded silica supported MoO_3 (<0.5 atom Mo/nm^2) to those reported here have been reported by four groups [1,5,11,12], and a one-peak reduction pattern of low loaded samples is reported in refs. [1,11]. Refs. [1,5,12], however, ascribe the first peak to "monolayer" MoO_3, while the second peak is assigned to crystalline MoO_3. This mechanism can be thought of as a series single-step mechanisms, as opposed to the parallel, two-step process suggested above. The Thomas group [1] does allow that some of the crystalline MoO_3 reduces in the first reduction step. However, the present XRD data and that of ref. [11] confirm that the two-step reduction process is operative. In the last column of table 1, a consistent interpretation of the first four entries is suggested based on the parallel two-step process for polymolybdate and crystalline MoO_3 for the moderate and high loadings, and the first reduction step for polymolybdates at low loading.

Table 1
Comparison of MoO_3 TPR literature for silica supported catalysts

Ref., fig.	Bulk TPR	Supported TPR loading – # peaks	Interpretation [a]	Present interpretation [a]
this work	= mod or high loading	high – 2		$polyMoO_3 + crystMoO_3 \rightarrow MoO_2$, $MoO_2 \rightarrow Mo$
		mod – 2		$polyMoO_3 \rightarrow MoO_2$, $MoO_2 \rightarrow Mo$
		low – 2+		$polyMoO_3 \rightarrow MoO_x$,?
[1] fig. 1	≈ peak 2 of high loading	high – 2	$monolMoO_3 \rightarrow Mo + crystMoO_3 \rightarrow MoO_2$, $crystMoO_3 + MoO_2 \rightarrow Mo$	$polyMoO_3 + crystMoO_3 \rightarrow MoO_2$, $MoO_2 \rightarrow Mo$
		mod – 2	$monolMoO_3 \rightarrow Mo + crystMoO_3 \rightarrow MoO_2$, $crystMoO_3 + MoO_2 \rightarrow Mo$	$polyMoO_3 \rightarrow MoO_2$, $MoO_2 \rightarrow Mo$
		low – 1	$monolMoO_3 \rightarrow Mo$	$polyMoO_3 \rightarrow MoO_2$
[5] fig. 1	–	high – 2	$monolMoO_3 \rightarrow Mo$ $crystMoO_3 \rightarrow Mo$	$polyMoO_3 \rightarrow MoO_2$, $MoO_2 \rightarrow Mo$
		mod – 2	$monolMoO_3 \rightarrow Mo$ $crystMoO_3 \rightarrow Mo$	$polyMoO_3 \rightarrow MoO_2$, $MoO_2 \rightarrow Mo$
[12] fig. 3	varies with loading [19]	high – 2	$monolMoO_3 \rightarrow Mo + crystMoO_3 \rightarrow MoO_2$, $MoO_2 \rightarrow Mo$	$polyMoO_3 + crystMoO_3 \rightarrow MoO_2$, $MoO_2 \rightarrow Mo$
[11] fig. 3	much higher than sup'd	high – 2	$MoO_3 \rightarrow MoO_2$, $MoO_2 \rightarrow Mo$	$polyMoO_3 + crystMoO_3 \rightarrow MoO_2$, $MoO_2 \rightarrow Mo$
		mod – 2	$MoO_3 \rightarrow MoO_2$, $MoO_2 \rightarrow Mo$	$polyMoO_3 \rightarrow MoO_2$, $MoO_2 \rightarrow Mo$
		low – 1	$MoO_3 \rightarrow MoO_2$	$polyMoO_3 \rightarrow MoO_2$
[6] figs. 4, 6	sl. higher than sup'd peaks 2, 4	high – 4	$cryst_1MoO_3 \rightarrow MoO_2$, $cryst_2MoO_3 \rightarrow MoO_2$, $cryst_1MoO_2 \rightarrow Mo$, $cryst_2MoO_2 \rightarrow Mo$	$polyMoO_3 + crystMoO_3 \rightarrow MoO_2$, $(blkMoO_3 \rightarrow MoO_2)$, $polyMoO_3 + crystMoO_2 \rightarrow Mo$, $(blkMoO_2 \rightarrow Mo)$
		mod – 4		
[7] fig. 2	much higher than sup'd	high – 2(4)	pH 1: $SiMoO_x$: $Mo^{VI} \rightarrow Mo^{IV}$, $SiMoO_x$: $Mo^{IV} \rightarrow Mo^0$, pH 6: $crystMoO_3 \rightarrow MoO_2$, $SiMoO_x$: $Mo^{VI} \rightarrow Mo^{IV}$, $crystMoO_2 \rightarrow Mo$, $SiMoO_x$: $Mo^{IV} \rightarrow Mo^0$	$poly + crystMoO_3 \rightarrow MoO_2$, $MoO_2 \rightarrow Mo$
				$polyMoO_3 + crystMoO_3 \rightarrow MoO_2$, $blkMoO_3 \rightarrow MoO_2$, $polyMoO_3 + crystMoO_2 \rightarrow Mo$, $blkMoO_2 \rightarrow Mo$
			pH 11: $SiMoO_x$: $Mo^{VI} \rightarrow$?, $crystMoO_3 \rightarrow MoO_2$, $MoO_2 \rightarrow Mo$	$blkMoO_3 \rightarrow MoO_2$, $blkMoO_2 \rightarrow Mo$
[8] fig. 3	much higher than sup'd	high – 4?	$monolMoO_3 \rightarrow Mo$, multi + $crystMoO_3 \rightarrow Mo$, ?, ?	$poly + crystMoO_3 \rightarrow MoO_2$, $bulkMoO_3 \rightarrow MoO_2$, $MoO_2 \rightarrow Mo$
[10] fig. 8	–	high – 3	$polyMoO_3 \rightarrow MoO_2$, $crystMoO_3 \rightarrow$?, $MoO_2 \rightarrow Mo$	$poly + crystMoO_3 \rightarrow MoO_2$, $bulkMoO_3 \rightarrow MoO_2$, $MoO_2 \rightarrow Mo$
		mod – 3	$polyMoO_3 \rightarrow MoO_2$, SM → ?, $MoO_2 \rightarrow Mo$	

[a] monol = monolayer, multi = multilayer SM or $SiMoO_x$ = silicomolybdic species, monom = monomeric, poly = polymolybdate, cryst = supported crystallites, blk = bulk (unsupported crystals), sup'd = supported.

In the last four entries of table 1 [6–8,10], three- and four-peak MoO_3/SiO_2 patterns are reported in which the main characteristic is an extra peak between the two peaks of the "normal" pattern. The extra peaks might be ascribed to the presence of not a second type of supported crystalline MoO_3 as suggested in ref. [6], but bulk MoO_3, which can form during catalyst preparation if the Mo/SiO_2 slurries are not well mixed during drying [23,26]. The migration and segregation of Mo in SiO_2 slurries during drying has been studied in detail [26]. The migration occurs because Mo species are not adsorbed by SiO_2 and, remaining in the liquid phase, are convected to the exterior surface of particles as drying occurs. Segregated AHM converts to bulk MoO_3 after calcination and can be seen as a light green layer. If this sample is reduced after being only poorly homogenized, a combination of the pattern for the poorly mixed sample, fig. 1, pattern (c) which included a peak at intermediate temperature, would be coadded to the two-peak pattern of the polymolybdate reduction. If a great deal of segregation had occurred in a sample, such that the remaining MoO_3 loading on SiO_2 was too low to completely reduce, and if the sample was thoroughly homogenized, the patterns for "well mixed" diluted MoO_3 and the single peak profile characteristic of low loading MoO_3/SiO_2 would be coadded. This would result in a two-peak pattern in which the area for the first peak would be greater than the 1 : 2 ratio to the second peak normally expected for moderate or higher loadings.

Several experimental conditions in refs. [6–8] point to the assignment of the first reduction step of bulk MoO_3 to the central peak. First of all, the sample used to produce pattern d of fig. 3 in ref. [8], which contains a prominent central peak, was certainly an unredispersed physical mixture. Secondly, refs. [6,7] both show the same trend in the central peak area with pH (fig. 4 of ref. [6] and fig. 2 of ref. [7]): the central peak area increases as pH decreases. At lower pH, MoO_3 is more soluble in water, such that during drying, more molybdates would remain in solution and be segregated to the surface of particles or the powder bed, forming more bulk MoO_3 upon calcination. The same assignment might be made for the central peak of fig. 8 in ref. [10], but this assignment is perhaps the most tenuous.

With the inclusion of a bulk MoO_3 species resulting from known segregation behavior, a consistent interpretation is offered in table 1 for all data sets. This interpretation consists of a parallel, simultaneous two-step reduction process for polymolybdates and crystalline MoO_3 at moderate and high loadings, only the first step of reduction for low loading polymolybdates, and a centrally located first reduction step of bulk MoO_3 in segregated MoO_3/SiO_2 samples. Four-peak patterns could also contain a slightly displaced bulk $MoO_2 \rightarrow Mo$ peak at high temperature.

While it appears that silica supported polymolybdates and MoO_3 crystallites and even well diluted bulk MoO_3 reduce at about the same temperature, morphology might be revealed from the width of the first reduction peak. In fig. 7 a decrease in the peak widths occurs with increasing particle size, as claimed in other works ([1] and citations therein). In this work the trend is supported from XRD

data (fig. 5). A comprehensive correlation of XRD peak broadening, chemisorption and width of the first reduction peak is reported for the present series of orthorhombic samples as well as for a series of sintered hexagonal and well dispersed hexagonal catalysts for methanol oxidation [27].

Reduction patterns for the alumina supported samples are shown in fig. 8, and alumina supported MoO_3 TPR literature is summarized in table 2. Although complete reduction is not evident in the TPR patterns, only crystalline Mo^0 and minor peaks from alumina appear in the XRD patterns of the 1000°C reduced samples (fig. 4). The intermediate phase, from runs stopped at 650°C, is MoO_2 (fig. 3). Thus the alumina supported samples also undergo a parallel two-step reduction process. However, the reduction of different species does not appear to be simultaneous as in the case of silica. First of all, in fig. 8 it is observed that the first reduction peak of the well mixed diluted sample (pattern (f)) lines up with the second peak of the 6 and 12 atoms Mo/nm^2 samples at about 540°C. The area of this second peak correlates with the fraction of MoO_3 crystallites as seen by XRD in fig. 6. Therefore, the second peak is assigned to supported MoO_3 crystallite reduction to MoO_2, while the first peak at about 490°C is assigned to polymolybdate reduction to MoO_2. (Again, the polymolybdate species on alumina undergo dehydration, to a combination of isolated mon-oxo species and some polymeric species [28] at elevated temperature, and it is probably these that reduce.) Precisely the same assignments, and nearly identical patterns have been reported for a series of MoO_3/Al_2O_3 samples thoroughly characterized by Raman spectroscopy [9]. Similar patterns for the corresponding weight loadings, including the second peak, were reported by Thomas [2], but no assignment was made for this peak (4.48 atoms Mo/nm^2 loading pattern of fig. 2). Two other works, refs. [6,12], also show similar patterns and make the same peak assignment for crystalline MoO_3 on the basis of XRD characterization. In another work, this peak increased markedly at conditions where sintering and formation of crystalline MoO_3 would occur (ref. [8], patterns g and f of fig. 3), although it was assigned to a more dispersed form of MoO_3.

The width of the diluted bulk sample (pattern (f), fig. 8) appears to be somewhat narrower than the second reduction peak of the high loading supported sample (pattern (e), fig. 8). The trend of increasing peak width with decreasing particle size might also be suggested for crystalline MoO_3 over alumina, although it is less clear than for the silica supported samples.

While the precise positions of T_{max} for the different peaks varied from study to study depending on TPR conditions, a consistent difference in T_{max} between the first reduction peak for alumina and silica supported samples, assigned here to the respective supported polymolybdate species, is seen in the literature. This difference is given in table 3. The reduction of the polymolybdate over alumina consistently occurs at about 80°C lower than over silica. This reduction temperature decrease of the polymolybdate species on alumina with respect to silica, and polymolybdate with respect to crystalline MoO_3 on alumina, indicates that stronger

Table 2
Comparison of MoO_3 TPR literature for alumina supported catalysts

Ref., fig.	Bulk TPR	Supported TPR loading–# peaks	Interpretation[a]	Present interpretation[a]
this work fig. 10	≈ sup'd high loading peaks 2, 3	high–3 mod–2 low–1+		$polyMoO_3 \rightarrow MoO_2$, $crystMoO_3 \rightarrow MoO_2$, $MoO_2 \rightarrow Mo$ $polyMoO_3 \rightarrow MoO_2$, $(MoO_2 \rightarrow Mo)$ $polyMoO_3 \rightarrow MoO_2$, $monomMoO_3 \rightarrow Mo + MoO_2 \rightarrow Mo$
[2] figs. 2, 3, 4	≈ peak 3 of sup'd high loading	high–3 mod–2 low–1	$multiMoO_3 \rightarrow Mo$, ?, $monolMoO_3 \rightarrow Mo$ $multiMoO_3 \rightarrow Mo$, $monolMoO_3 \rightarrow Mo$ $monolMoO_3 \rightarrow Mo$	$polyMoO_3 \rightarrow MoO_2$, $crystMoO_3 \rightarrow MoO_2$, $MoO_2 \rightarrow Mo$ $polyMoO_3 \rightarrow MoO_2$, $MoO_2 \rightarrow Mo$ $monomMoO_3 \rightarrow Mo$
[3] fig. 3	–	high–2 mod–2	$Mo(T) + Mo(O) \rightarrow Mo^{4+}$, $Mo^{4+} \rightarrow Mo$ $mo(T) + Mo(O) \rightarrow Mo^{4+}$, $Mo^{4+} \rightarrow Mo$	$polyMoO_3 \rightarrow MoO_2$, $MoO_2 \rightarrow Mo$ $polyMoO_3 \rightarrow MoO_2$, $MoO_2 \rightarrow Mo$
[5] fig. 1	–	high–2 mod–2	$multiMoO_3 \rightarrow Mo$, $monolMoO_3 \rightarrow Mo$ $multiMoO_3 \rightarrow Mo$, $monolMoO_3 \rightarrow Mo$	$polyMoO_3 \rightarrow MoO_2$, $MoO_2 \rightarrow Mo$ $polyMoO_3 \rightarrow MoO_2$, $MoO_2 \rightarrow Mo$
[6] figs. 4a, 5	much higher than sup'd	high–2 (3) mod–2	$multi + polyMoO_3 \rightarrow MoO_2$, $(crystMoO_3 \rightarrow Mo)$, $MoO_2 \rightarrow MoO_x$ $multi + polyMoO_3 \rightarrow MoO_2$, $MoO_2 \rightarrow MoO_x$	$polyMoO_3 \rightarrow MoO_2$, $crystMoO_3 \rightarrow MoO_2$, $MoO_2 \rightarrow Mo$ $polyMoO_3 \rightarrow MoO_2$, $MoO_2 \rightarrow Mo$
[8] fig. 3	much higher than sup'd	high–3 (4?)	$multiMoO_3 \rightarrow Mo$, $monolMoO_3 \rightarrow Mo$, $crystMoO_3 \rightarrow Mo$	$polyMoO_3 \rightarrow MoO_2$, $crystMoO_3 \rightarrow MoO_2$, $MoO_2 \rightarrow Mo$
[9] fig. 3	much higher than sup'd	high–3 mod–2	$polyMoO_3 \rightarrow MoO_2$, $(crystMoO_3 \rightarrow Mo?)$, $MoO_2 \rightarrow Mo$ $polyMoO_3 \rightarrow MoO_2$, $MoO_2 \rightarrow Mo$	$polyMoO_3 \rightarrow MoO_2$, $crystMoO_3 \rightarrow MoO_2$, $MoO_2 \rightarrow Mo$ $polyMoO_3 \rightarrow MoO_2$, $MoO_2 \rightarrow Mo$
[4] fig. 3	≈ peak 3 of sup'd	mod–3 low-mod–2	capping O, surface O, blk O capping O, surface O	$polyMoO_3 \rightarrow MoO_2$, $crystMoO_3 \rightarrow MoO_2$, $MoO_2 \rightarrow Mo$ $polyMoO_3 \rightarrow MoO_2$, $MoO_2 \rightarrow Mo$
[7] fig. 3	2nd peak ≈ 2nd sup'd pk.	mod–2	?, mixed MoO_3–$Al_2O_3 \rightarrow Mo$	$polyMoO_3 \rightarrow MoO_2$, $MoO_2 \rightarrow Mo$ $polyMoO_3 \rightarrow MoO_2$, $MoO_2 \rightarrow Mo + monomMoO_3 \rightarrow Mo$
[12] fig. 1	varies with loading [19]	high–3 low-mod–2	$multiMoO_3 \rightarrow Mo$, $crystMoO_3 \rightarrow Mo$, $monom + polyMoO_3 \rightarrow Mo$ $multiMoO_3 \rightarrow Mo$, $monom + polyMoO_3 \rightarrow Mo$	$polyMoO_3 \rightarrow MoO_2$, $crystMoO_3 \rightarrow MoO_2$, $MoO_2 \rightarrow Mo$ $polyMoO_3 \rightarrow MoO_2$, $(MoO_2 \rightarrow Mo + monomMoO_3 \rightarrow Mo)$

[a] monol = monolayer, multi = multilayer, monom = monomeric, poly = polymolybdate, cryst = supported crystalline, sup'd = supported.

Table 3
Initial peak T_{max} difference between Al_2O_3 and SiO_2

Ref.	T_{max}		Difference (K)
	Al_2O_3	SiO_2	
[1,2]	650 K	720 K	70
[5]	≈ 530°C	≈ 600°C	70
[6]	410°C	490°C	80
[7]	450°C	550°C	100
[8]	765 K	850 K	85
[12]	650 K	730 K	80
this work	480°C	560°C	80

support interaction results in a *lower* reduction temperature, in contradiction to the majority of the literature. This point will be discussed further momentarily.

A final, high temperature reduction peak is seen at the lowest loadings in this work (second peak of pattern (b) of fig. 8) and at low loadings in other works [2,4,12]. Only this high temperature peak, at greater than 1000 K, is seen at very low loadings [2]. The peak has traditionally been assigned to a "monolayer species" and this assignment remains as loading increases and the final peak temperature shifts downward several hundred degrees C (ref. [2] and citations therein).

This peak can be assigned to the monomeric species (or more accurately, the dehydrated form of it), which exists at loadings low enough that the area weighted isoelectric point is still close to the isoelectric point of alumina, that is, in the pH range where the monomer MoO_4^{2-} species predominates [19]. The loading limit at which the monomeric form predominates is 1 atom Mo/nm^2, while between 1 and 2 or 2.5 atoms Mo/nm^2, both species coexist [19]. The first peak of the 0.2 atom/nm^2 sample, pattern (b) of fig. 8, is assigned to the first reduction step of a relatively small fraction of polymolybdate, and the second to a sum of the reduction of polymolybdate MoO_2 to Mo and the total reduction of monomeric MoO_3.

Two interesting discrepancies occur between the reduction behavior of this species and the polymolybdate species. First of all, the monomeric species seems to reduce all at once ($MoO_3 \rightarrow Mo$). Secondly, the higher reduction temperature contradicts the trend just stated that stronger interaction leads to lower reduction temperatures. It is tempting to explain both of these contradictions by the reduction mechanism of Arnoldy [21], applied to supported MoO_3 species. Monomeric species, by virtue of their isolation, cannot undergo low temperature, autocatalytic reduction. Thus the monomeric species must utilize the high temperature reduction pathway, as does water inhibited bulk MoO_3 [21]. The increased reduction temperature then stems not from a stronger interaction, but from a different reduction pathway. This species never forms over silica [18], and a reduction peak at this high temperature is not seen except for the inhibited bulk samples. In formulating this explanation it is assumed that even while the microscopic environment of the dehydrated mono-oxo species is spread relative to its polymeric hydrated form

[25,28], the dehydrated Mo units are still in close enough proximity to autoreduce. The mono-oxo units derived from the low loading alumina samples would be well dispersed due to their initial deposition as MoO_4^{2-}.

A relatively consistent interpretation can be rendered from the various studies of MoO_3/Al_2O_3 TPR, as listed in table 2. For high and moderate loadings [2,3,5,6, 8,9,12], the first peak corresponds to polymolybdate → MoO_2, and at the highest loadings a second (sometimes shoulder) corresponds to crystalline MoO_3. The third peak is that for MoO_2 → Mo. One other work has made the same assignments [9], as mentioned earlier. Another work invokes the same two-step reduction process, but claims both tetragonal and octahedral species undergo it in parallel [3]. Some works assign the high temperature peak of high loadings to the "monolayer" form [2,5,12], on the basis that the high temperature peak at low loadings smoothly shifts down in temperature at the high loadings.

Several sets of data, for lower loadings, can be ascribed to a mixture of monomeric and polymolybdate species, and show one small peak at low temperature, and a much larger one at very high temperature [2,7,12] as in pattern (b) of fig. 8. Experiments were run at higher loadings in refs. [2,12] and in both cases a 1 : 2 area ratio was approached at the higher loadings where polymolybdate would be formed in entirety. Finally, the single high temperature peak for very low loadings observed in ref. [2] is assignable to monomeric MoO_3. The assignment of the high temperature peak to "monolayer" MoO_3 at low loadings [2] is correct (this species is now identified as monomeric), but the assignment changes at higher loadings for the peak several hundred degrees lower, to the second reduction step of all species. Many works have maintained the monolayer assignment to the higher loading, lower temperature peak [2,5,8,12].

One of the main findings of this work is that diluted bulk MoO_3 actually reduces at the same temperature as supported crystalline MoO_3, and in the case of silica, also at the same temperature as polymolybdates. In virtually every comparison of the reduction of bulk to supported MoO_3, over silica [1,11,6–8] or alumina [2,6,8,9,4,7], the bulk phase is reported to reduce at higher or much higher temperatures, and the conclusion is drawn that the supported crystallites are much better dispersed than the bulk material. This inference is demonstrated to be invalid by these results; relative crystal size can be seen, however, with the width of the first reduction peak for silica, and the second reduction peak for alumina. The implication with regard to catalytic activity that crystalline MoO_3 will undergo a redox cycle more readily than bulk MoO_3 is therefore misleading, if the cycle does not produce water. The redox capacity of well dispersed MoO_3 on silica (polymolybdates) should also roughly be the same as for crystallites. Only over alumina do the different species appear to have different redox capacities, and in the order polymolybdate > crystalline MoO_3 > monomeric MoO_3.

There are also implications of this work regarding the O_2 chemisorption technique. The first reduction step, normally a prolonged reduction at 500°C, may be appropriate for supported samples. As suggested by de Boer [11] as well as the pres-

ent results, however, a better technique would be individually tailoring the first reduction step by monitoring the reduction progress. In studies of bulk MoO_3, the 500°C calcination might very often be inadequate and result in an underestimation of chemisorption capacity; the remedy to this is simply to dilute the bulk sample in a silica, alumina, or perhaps other support.

Finally, the results for MoO_3 over silica and alumina might cautiously be extended to other supports and oxides. Bulk MoO_3 has been reported to reduce at much higher temperatures than titania supported MoO_3 [13,14], and this is also the case for bulk and supported vanadia over titania [16,17]. Dilution experiments appear to reveal a more representative reduction pattern of the bulk oxide, and in doing so assist the assignment of TPR patterns in those systems.

4. Summary

Experiments in which bulk MoO_3 has been diluted in silica or alumina have shown that the bulk oxide reduces at the same temperature as the supported crystalline phase when placed in roughly the same physical surroundings as the supported crystallites. Diluted samples appear to manifest the low temperature autocatalytic reduction mechanism postulated by Arnoldy and coworkers [21], by virtue of the dilution and more efficient removal of water vapor. The reduction patterns for diluted bulk MoO_3, in conjunction with an XRD study of the reduction process and the recent comprehensive speciation theory of Wachs [18–21], has greatly assisted the assignment of peaks for silica and alumina supported samples. A simple interpretation of TPR patterns has been applied with good agreement to the body of MoO_3 TPR literature; with a consistent interpretation, temperature programmed reduction might be employed with increased confidence to characterize supported MoO_3 and perhaps other supported oxides.

References

[1] R. Thomas et al., J. Catal. 84 (1983) 275.
[2] R. Thomas et al., J. Catal. 76 (1982) 241.
[3] C.V. Caceres et al., J. Catal. 95 (1985) 501.
[4] H.C. Yao, J. Catal. 70 (1981) 440.
[5] J. Brito and J. Laine, Polyhedron 5 (1986) 179.
[6] R. Lopez Cordero, F.J.G. Llambias and A.L. Agudo, Appl. Catal. 74 (1991) 125.
[7] H.M. Ismail et al., Appl. Catal. 72 (1991) L1.
[8] M. del Arco et al., J. Mater. Sci 27 (1992) 2960.
[9] M. del Arco et al., J. Catal. 141 (1993) 48.
[10] M.R. Smith et al., Catal. Lett. 9 (1993) 1.
[11] M. de Boer, PhD dissert., University of Utrecht, The Netherlands (1992) ch. 6.
[12] P. Arnoldy, PhD dissert., University of Amsterdam, The Netherlands (1985) ch. 5.
[13] G.C. Bond, S. Flamerz and L. van Wijk, Catal. Today 1 (1987) 229.

[14] M. del Arco et al., J. Chem. Soc. Faraday Trans. 89 (1993) 1071.
[15] P. Arnoldy and J.A. Moulijn, J. Catal. 83 (1985) 38.
[16] G.C. Bond and A.F. Tahir, Appl. Catal. 71 (1991) 1.
[17] F. Roozeboom et al., J. Phys. Chem. 84 (1980) 2783.
[18] C.C. Williams et al., J. Phys. Chem. 95 (1991) 8781.
[19] C.C. Williams et al., J. Phys. Chem. 95 (1991) 8791.
[20] G. Deo and I.E. Wachs, J. Phys. Chem. 95 (1991) 5889.
[21] I.E. Wachs et al., J. Mol. Catal. 82 (1993) 443.
[22] P. Arnoldy, J.C.M. de Jonge and J.A. Moulijn, J. Phys. Chem. 89 (1985) 4517.
[23] A. Datta and J.R. Regalbuto, J. Catal. 133 (1992) 55.
[24] D.A.M. Monte and A. Baiker, J. Catal. 83 (1993) 323.
[25] M. de Boer et al., Catal. Lett. 11 (1991) 227.
[26] N. Santhanam et al., Catal. Today, in press.
[27] J.-W. Ha and J.R. Regalbuto, in preparation.
[28] M.A. Vuurman and I.E. Wachs, J. Phys. Chem. 96 (1992) 5008.